REVIEW ARTICLE

Prepreg tack: A review of mechanisms, measurement, and manufacturing implication

Dennis Budelmann[1] 🔟 | Carsten Schmidt[2] | Dieter Meiners[3]

[1]Institute of Polymer Materials and Plastics Engineering, Clausthal University of Technology, Stade, Germany

[2]Institute of Production Engineering and Machine Tools, Leibniz Universität Hannover, Stade, Germany

[3]Institute of Polymer Materials and Plastics Engineering, Clausthal University of Technology, Clausthal-Zellerfeld, Germany

Correspondence
Dennis Budelmann, Institute of Polymer Materials and Plastics Engineering, Clausthal University of Technology, Ottenbecker Damm 12, Stade, Germany.
Email: dennis.budelmann@tu-clausthal.de

Abstract

The stickiness of prepregs (tack) is considered a decisive material property for the success of high-quality composite manufacturing by automated lay-up processes such as automated fiber placement (AFP) or automated tape laying (ATL). Adverse control of prepreg tack can easily result in laminate defects or machine breakdown, which are highly undesirable considering the tremendous machinery and material costs of these processes. Prepreg tack is governed by a complex interaction of adhesive and cohesive phenomena that are influenced by machine and environmental parameters of the production process as well as by intrinsic properties of the prepreg material itself. This review aims at providing a condensed insight into the current state of research on prepreg tack. Therefore, experimental studies including the discussion of utilized tack measurement methods as well as model approaches to prepreg tack are reviewed. The findings are discussed against the background of fundamental mechanisms, the strong interdependency of influencing parameters and the challenge of translating measured tack data into an enhanced AFP/ATL process stability by process adjustment.

KEYWORDS

adhesion, cohesion, composites, interfaces, processing

1 | INTRODUCTION

Lightweight construction based on carbon fiber reinforced plastics has evolved into a key technology to achieve both the economic and ecological mobility goals of modern civil aviation.[1,2] Large-scale composite parts with the highest level of mechanical performance are manufactured by automated lay-up of epoxy preimpregnated carbon fibers and subsequent autoclave cure.[3,4] The most prevalent processes automated fiber placement (AFP) and automated tape laying (ATL) employ robot- or gantry-attached endeffectors, which build up an uncured laminate ply-by-ply on the surface of a rigid tool.[5,6] Automated lay-up technology has substantial benefits compared to the hand laminating of prepreg material in terms of both the quality and productivity with the most prevalent being higher output volume,[7] ply placement accuracy in terms of repeatability[8,9] and uniform laminate compaction.[10] In order to maintain it in the desired position, the material laid must provide a certain level of stickiness,[11] commonly referred to as prepreg tack. In combination with drape, tack is the most important material property of the prepreg material for a successful outcome of automated processing using lay-up technology.[12]

There is no well-established definition of prepreg tack as a material property specifying its predominating mechanisms or stipulating how to quantify it. Still, it can be generally stated that prepreg tack phenomenologically is not an effect of the epoxy cure reaction forming covalent bonds to a substrate but can rather be understood as an intrinsic stickiness in the absence of any chemical reactions or solvent evaporation. In this regard, it is basically similar to pressure sensitive adhesives (PSA) which have been the target of extensive scientific research for several decades since their economic breakthrough in the late 19th century.[13] For both thermoset prepregs and PSA, tack is a measure of mechanical resistance that needs to be overcome in order to separate the prepreg/adhesive and the substrate. Characteristically, the intimate interfacial contact between both bonding partners is established by applying light pressure over a short period of time compared to most physically or chemically setting structural adhesives.[14,15] Despite all the similarities between prepreg and PSA tack, both the process-related framework of AFP/ATL and the peculiarity of prepregs (presence of reinforcement fibers, B-stage, etc.) must be taken into account for prepreg tack characterization. This makes prepreg tack a complex phenomenon governed by adhesive and cohesive mechanisms which themselves are strongly affected by a large set of influence parameters. As individual research papers are forced to selectively focus on individual aspects of the topic's complexity (for example, isolated influence parameters), it can be a challenge to fully comprehend the nature of prepreg tack. As well as giving a brief overview of the topic, this article summarizes the fundamentals of prepreg tack by reviewing the most common methods of quantification, results and deductions based on experimental characterization as well as modeling approaches presented in literature. The challenge of transferring measurement and simulation results into the practice of automated composite manufacturing and, finally, topics to be covered in future research are presented.

2 | ROLE OF PREPREG TACK IN AFP/ATL

The beginning of scientific research on prepreg tack can be dated back to the early 1980s[16] - a period of time in which AFP and ATL systems gained increasing technical maturity as a consequence of technological innovation[17–19] and, subsequently, established its first industrial relevance. The strong interest in automated lay-up technology from this point in time on can also be retraced to the increasing publication output highlighted in the review article by Lukaszewicz et al.[20] Evidently, providing robust processes was inevitably linked to the necessity of quantifying prepreg tack from the very beginning of technology refinement.

2.1 | General process considerations

Figure 1 illustrates the ATL process with regard to the adhesive interaction between prepreg material (including backing paper), lay-up surface, and different machine elements. Dark arrows indicate prepreg tack whereas counteracting forces are displayed in white.

With the help of the simplified force diagram, it makes sense that optimum tack does not equal maximum tack from a processing perspective by any means. Actually, a suitable level of prepreg tack is a sensible balance between partially conflicting requirements: On the one hand, tack needs to be preferably low on its way through the placement head prior to the nip point in order not to adhere to guiding or conveying elements such as the material feed rollers (Figure 1A). Resin gradually building up around the cutting unit can also cause material jams because of resin adhering to the blades (Figure 1B). On the other hand, high tack is required to keep the laid prepreg material in position by withstanding peel forces that result from the removal of the backing paper (Figure 1C). For AFP, the adhesive interaction of the slit tape with the compaction roller is crucial if the release film has been removed before compaction. Successful lay-up at the nip point is achieved for both processes if the adherence of prepreg toward the substrate is higher than toward the backing paper/compaction roller. Otherwise, the material will either be removed right after lay-up by the placement head or defect formation will occur within the laminate.

2.2 | Production-induced defects

Various types of lay-up defects are known to occur during automated lay-up, namely, positioning defects such as
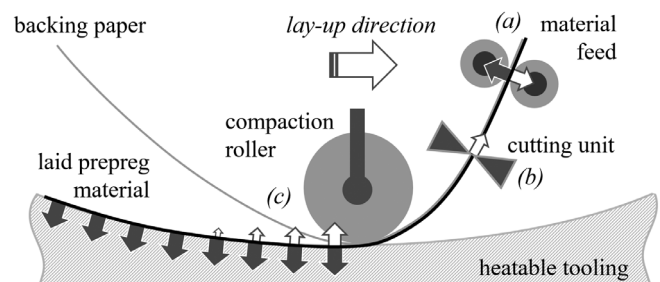

FIGURE 1 Schematic representation of prepreg tack in automated tape laying (ATL) processes. Adapted from ref. [21] with permission from Elsevier, 2012, and extended by authors

gaps, overlaps or twisted tows[22–26] and bonding defects such as wrinkles/buckles, bridging, or pull-ups at tow ends.[27,28] Depending on their occurrence in terms of type, size, and frequency, production-related defects have been found to affect the mechanical properties even after autoclave cure.[29–33]

If not handled adequately, unfavorable tack, in particular, can be responsible for the formation of the aforementioned bonding defects. One type of defect that has been investigated extensively is out-of-plane wrinkles as a result of tow steering. If prepreg tows are placed along curved paths, a mismatch between fiber length and steering path arises.[34] In-plane compressive stress on the tow inside results in buckling which counteracts the adhesive forces of prepreg tack holding down the tow (Figure 2B). Wrinkles can be observed when the steering radius reaches a critical minimum.[35] A number of studies have examined the minimum steering radius of defect-free lay-up experimentally.[11,36–38]

In some research papers, models are presented that directly include the role of prepreg tack. Bakjshi and Hojjati[35] introduced a time-dependent buckling model for an orthotropic plate resting on a generalized viscoelastic Pasternak foundation. With the help of the model and experimental data from tack measurement, the authors are able to predict the length of wrinkles and their formation as a function of time. Lichtinger et al.[39] use a theoretical relationship between tack and compaction considerations[40] in order to predict gaps and bridging. Bridging occurs in concave mold sections to reach lower energy levels if tensile stress exceeds tack[36] and eventually lifts the material laid (Figure 2A). Tensile stress of the material laid can often be controlled as a process parameter or is induced as a result of underdosed material feed and at steering as discussed above. Another bonding defect-inducing scenario becomes a reality when high prepreg stiffness leads to material pull up, for example, on convex surfaces (Figure 2C).

For automated prepreg processing by lay-up, both scenarios of machine downtime, manual laminate repair due to defects and or even wastage production are highly undesirable as they have serious economic repercussions given the high machinery (several million dollars[41]) and material costs (>100 dollars/kg[42]). Productivity issues for AFP are ascribed to machine downtime reported of up to 50%.[43] The potential of AFP and especially ATL to excel as the most cost-effective automated composite manufacturing processes for selected industries (as demonstrated in refs. [44], [45], and [46]) is, therefore, highly sensitive to prepreg tack.

2.3 | Manufacturing-relevant factors affecting prepreg tack

A seemingly practicable way to categorize the different influencing factors on prepreg tack is to classify them into AFP/ATL-related process parameters, environmental aspects of composite production and the prepreg material properties as delivered. Table 1 summarizes the most relevant factors according to the suggested categories. A brief description of the influence parameters in relation to manufacturing and/or the prepreg material has been added.

Apparently, this suggestion of classification is not and cannot be fully selective as interdependencies have been observed for many of the conceivable factor combinations, for example, increased material temperature at the nip point of the material decreases the prepreg matrix viscosity and will eventually affect the measured tack. The interdependencies are discussed in detail in Section 4. However, the list illustrates the large variety of influence factors and, therefore, reflects the huge prospect of factor variation when characterizing prepreg tack experimentally. The majority of the depicted process parameters (Table 1) can be adjusted as test parameters within the
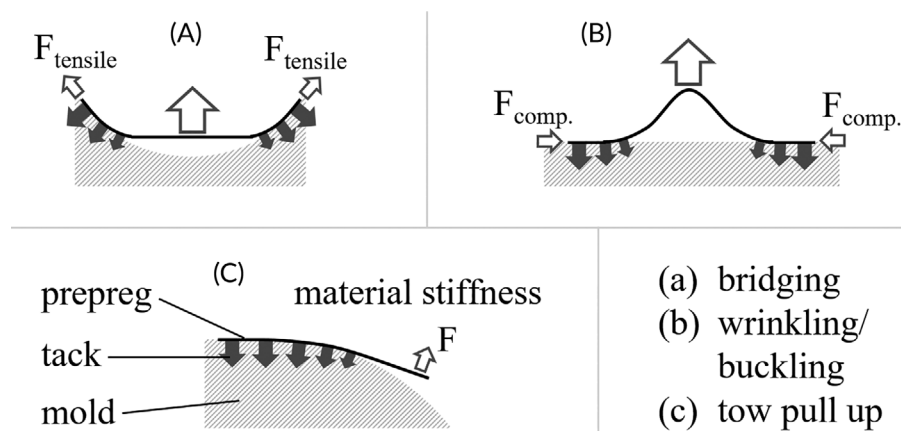

FIGURE 2 Tack-related defect formation in automated lay-up processes

TABLE 1 AFP/ATL-related influences on prepreg tack

Category	Influence parameter	Description
Process parameter (extrinsic)	Temperature	Prepreg, head, and mold temperature
	Compaction force	Pressure on material at nip point applied by compaction roller
	Compaction time	Duration of compaction (dependent on lay-up speed)
	Debonding rate	Defect/lay-up speed-dependent rate of prepreg removal from substrate
	Contact material	Surface material in contact with prepreg (mold, roller, backing paper, etc.)
Environmental factor (extrinsic)	Ageing	Material storage in and out of freezer due to proceeding cure reaction
	Relative humidity	Relative humidity in manufacturing environment causing moisture pickup
Material property (intrinsic)	Matrix viscosity	Epoxy resin flowability
	Prepreg architecture	Structural composition (impregnation level, tack-enhancing resin layers, etc.)
	FVF	Volumetric fiber/resin ratio
	DoC	Cured portion in initial B-stage as delivered

Abbreviation: AFP, automated fiber placement; ATL, automated tape laying; DoC, degree of cure; FVF, fiber volume fraction

measurement techniques for tack testing (Section 3) itself. Environmental aspects can be simulated artificially, for example, by material storage in climatic chambers prior to tack testing. Both process parameters and environmental factors are extrinsic influences on prepreg tack which are most relevant for prepreg processors in composite manufacturing. Influences of the third category, namely material properties, are considered intrinsic and accessible through standard material characterization in the form of rheological, thermal (cure kinetics, phase transitions, etc.), microscopic or wetting analysis. Prepreg manufacturers, in particular, can benefit from a deep understanding of prepreg tack's dependence on intrinsic material properties in order to supply tailor-made prepreg systems.

3 | MEASUREMENT

Given the high relevance of prepreg tack for advanced composite manufacturing by automated lay-up, it is rather surprising that prepreg data sheets have been providing very sparse information on tack properties to the present day. Information on tack is usually limited to the ordinal scaling of "low," "medium," or "high" and a declaration on how long the material will be sufficiently tacky, commonly referred to as tack life. In industrial practice, the adjustment of prepreg tack is thus mainly based on heuristic methods and experience rather than on measured data. Two aspects of prepreg tack characterization are primarily responsible for this:

- First, there is no standardized measurement technique to quantify the tack of resin impregnated fibers.[47] This failing seems to have gained recognition recently

as two test methods (ASTM WK67852 and WK70428) are being currently developed by the ASTM Committee.
- Second, prepreg tack is a complex phenomenon influenced by a multitude of parameters (see Section 4) which makes it impossible to break down tack properties to a single value. A whole set of test parameters has to be taken into account for comprehensive quantification.

Apart from industrial implications, both of these aspects have likewise been influencing the scientific activities on prepreg tack up to the present day. In order to tackle the first challenge, different measurement methods were utilized in the past. The majority of techniques have been adapted from PSA characterization due to their evident similarities in their fundamental adhesive nature. The methods are either performed according to PSA standards or are adapted and tailored to prepregs and/or lay-up process conditions. The methods utilized most often for experimental prepreg characterization are the probe tack test and peel test. Still, considerable research on comparability between different measuring techniques for tack testing of prepregs has not been conducted yet.

3.1 | Probe tack test

Probe tack testing is the mechanical simulation of the highly subjective thumb or finger tack test.[48] The test is standardized by ASTM D2979[49] which was withdrawn without a replacement in April 2019 due to its limited use in industry. However, it has been used extensively in PSA research[50–53] because of its precise control of input variables and high reproducibility[54] as well as its ability

to characterize the nature of debonding (cavitation and fibrillation) in detail.[55–57] The test, which is occasionally referred to as the Polyken (probe) test,[58] includes two strictly separate phases: During the compression phase, a flat probe is brought into contact with the tested material for a definite period of time (dwell time) under compressive force (Figure 3A). When the probe is removed at a controlled rate of separation during the tensile phase (Figure 3B), force is recorded as a function of displacement. Two main indicators for tack performance can be obtained from probe testing:

- Maximum force F_{max} during the debonding process, usually measured at low elongation in the early stages of separation.[59] If the separation force is divided by the contact area, a corresponding stress value σ_{max} can be calculated.
- The work of adhesion W_{adh} or fracture energy[60] describes the energy needed to separate the formed interface completely. It is calculated by taking the force integral over the displacement interval from the start of measurement to full separation ($F = 0$).[61]

The probe tack test is mainly performed by using fixtures mounted to universal testing machines. Heating chambers are applied for temperature-dependent testing. Most recently, rheometers were utilized for probe tack testing of prepreg materials as well.[62–64] Apart from the compression (Figure 3A) and tension/debonding phases (measurement, Figure 3B), Figure 3 also shows a characteristic force-displacement curve including its quantifiable tack indicators (Figure 3C). Dubois et al.[65] investigated the curve shape by probe tack testing prepreg. Phases known from PSA testing, namely cavity formation/growth and fibrillation,[66] were transferred to prepreg material and the differences between both materials were described in detail.

3.2 | Peel test

Several standards exist for testing the peel resistance of adhesives bonds.[67] Depending on the type of application, the standards differ in the applied peel angle (90° (Figure 3D[68]), 180°,[69] and T-Peel[70]) and/or in terms of the testing equipment employed, for example, by utilizing a floating roller (Figure 3E[71]) or a climbing drum.[72] ASTM 3330[73] provides several methods particularly designed for PSA tapes. All standards intend to remove progressively the tested material from a substrate or itself under a constant peel angle which results in the characteristic force/displacement curve depicted in the bottom right of Figure 3F. The most common approach to tack evaluation is to determine the average load throughout the measurement distance $F_\varnothing$. Alternatively or additionally, work of adhesion W_{adh} can be calculated similarly to the probe test described above. Adhesive peeling in general is a well-understood mechanism which has been the target of experimental and simulative studies for some time.[74–77]

3.3 | Other measurement techniques

Other standardized methods such as the loop tack (ASTM 6195[78]) or rolling ball method (ASTM D3121[79]) have not been utilized to quantify prepreg tack yet despite their common use in PSA testing.[80–83] However, efforts have been put into developing measurement techniques that mimic prepreg manipulation during AFP and ATL. Crossley et al. from the University of Nottingham present a modified peel test based on the floating roller method in ref. [84]. The method's applicability to prepreg was discussed in detail,[21] repeatedly utilized and refined for further experimental studies.[85–88] A large number of results gained with the help of the Crossley apparatus are
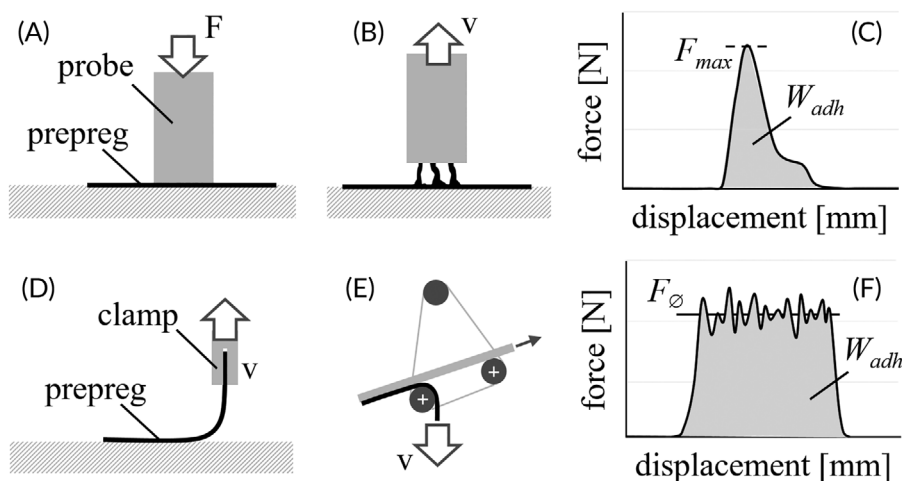

FIGURE 3 Upper figure: Compression, A, and tension/ measurement, B, phases in probe tack test; lower figure: 90°, D, and floating roller, E, peel test setups; right figure: Characteristic force/displacement curves, C, and, F

compiled in ref. [89], the only doctoral thesis exclusively dealing with prepreg tack known to the authors of this review article. The utilized test rig (Figure 4) mounted to a universal testing machine consists of two pairs of rollers with the first guiding the rigid plate. The second pair is spring-loaded and applies compaction force. When removing the prepreg material at a 90° peel angle, dynamic stiffness, and peel force are recorded over a pre-determined distance.

The authors argue that the measuring method developed reflects the ATL process more accurately than conventional tack testing methods due to the inverse correlation between contact time and peel rate. Furthermore, ATL process conditions are claimed to be simulated closer to reality in terms of lay-up speed and compaction force.[21]

Another manufacturing-inspired measurement method for prepreg tack is presented by Boeckl et al.[90,91] who developed an online monitoring system for slit tapes in AFP. The measurement principle differs significantly from conventional testing: The transverse friction force induced by the prepreg being forwarded through a loaded pair of rollers is used as a tack indicator. This way, prepreg tack can be measured continuously as a function of compaction force and the interdependent parameters prepreg velocity/contact time. The method shows the long-term potential of its implementation as an online quality control system in industrial practice due to its continuous mode of operation. It will, however, have to prove its validity by comparison to other methods like probe or peel testing first.

Nguyen performed tack characterization by producing overlapping (20 mm) prepreg specimens with the help of a robot-attached AFP head in a first step. The

specimens were then tested by using a self-designed lap shear fixture loosely based on ASTM D1002.[92] Employing the technique presented in ref. [93], testing of AFP-manufactured samples is possible. The method was modified and transferred into a fully robot-based measuring unit.[94]

4 | EXPERIMENTAL STUDIES

Experimental investigation of prepreg tack has been performed scientifically for almost four decades. The topic is still relevant in current research in the field of advanced composite manufacturing indicating that the nature of prepreg tack has not been fully understood yet. The preceding considerations can be retraced when looking at a chronological overview of performed experimental studies shown in Table 2. The table summarizes the findings for different input variables categorized according to the classification presented in Section 2.3. The response of the dependent variable prepreg tack is indicated for an increase in each input variable.

Several aspects of experimental prepreg characterization can be deduced from the tabular list. On the one hand, a slight focusing upon the investigation of process parameters is observed especially in the earliest studies. Applied research on finding solutions for processors to run stable processes appears predominant although a shift toward the investigation of prepreg tack fundamentals becomes apparent: Not much time passed until subsequent research started focusing on the more elaborate investigation of intrinsic material parameters on prepreg tack in order to gain a deeper understanding of the process-material interaction in AFP/ATL. In summary, the current state of research is a rather balanced compilation of studies on the influences of process parameters, environmental factors, and material properties on prepreg tack.

On the other hand, the large portion of complex tack responses (indicated by) that were found for the majority of input parameters is significant. For these cases, prepreg tack was found not to follow monotonically increasing/decreasing functions and/or showed significant interdependence with other input variables. The influence of temperature discussed in Section 4.1.1 can serve as a prime example of this behavior. In this context, Wohl et al. criticize experimental research that is conducted by investigating a single parameter of prepreg tack while the remaining parameters are kept constant. This necessarily eliminates the possibility of quantifying the influence of two (or more) parameters in conjunction with the property of interest.[62]
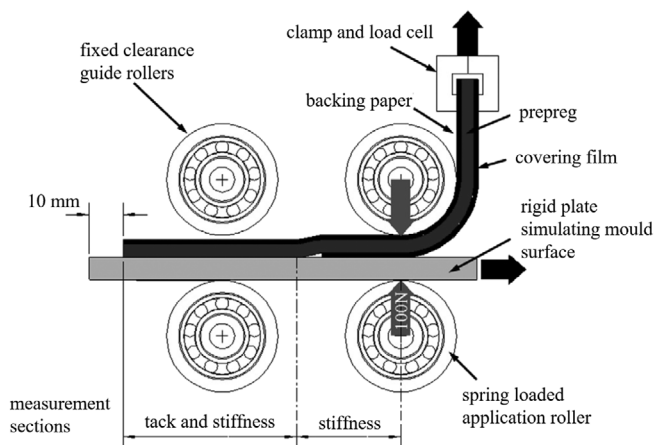

FIGURE 4 Crossley's peel tack and dynamic stiffness measuring equipment. Reprinted from ref. [86] with permission from Elsevier, 2013

TABLE 2 Overview of experimental studies of ATL/AFP-related influencing factors on prepreg tack

Ref./Year	Process parameter					Environmental factor		Material property				Test
	Temperature	Compaction force	Compaction time	Debonding rate	Contact surface	Ageing	Relative humidity	Viscosity	Architecture	FVF	DoC	
[64] 2019										(~)		Probe
[63] 2019	~	+		~	~	~		~	~		~	Probe
[88] 2018	~	+	~	~	~	−	+	~	~		−	Peel
[62] 2017	~	~	+	0			~	~				Probe
[94] 2017	(~)		0		~							Lap shear
[87] 2016	~		~	~	~				~			Peel
[95] 2016	+	~	~					~				Peel
[93] 2016	+					~		~				Lap shear
[86] 2013	~		~	~				~				Peel
[21] 2012	~		~	~				~	~	~		Peel
[85] 2011	~		~		~			~				Peel
[96] 2011								~			~	Peel
[97] 2011								~			~	Probe
[65] 2010	−	+	+	+		−			~		~	Probe
[98] 2004								~				Peel
[99] 2000									~			Probe
[100] 2000						−	~			−		Probe
[101] 1996	(−*)	(−*)							~			Probe
[102] 1995	(−*)		(−*)						~	−		Probe
[103] 1992	~					~		~	~		~	Probe
[104] 1992	~	+	+	+					~			Probe
[105] 1992	~	+	+	+		−					~	Probe
[106] 1991						(−)				~		Hold time
[16] 1981	~	+	+	+					(~)			Probe

Note: Key: [+] tack-increasing, [−] tack-decreasing, [~] complex tack response, [0] no significant influence, [()] limited validity, [ ] not investigated [*] varied during impregnation.
Abbreviations: AFP, automated fiber placement; ATL, automated tape laying; DoC, degree of cure; FVF, fiber volume fraction.

—WILEY—

4.1 | Process parameters

In the following subsections, the influences on prepreg tack are reviewed and discussed in detail. The authors of this review article desist from compiling a tabular overview of numerical prepreg tack data because direct comparison turns out to be problematic due to differences in measurement techniques, test parameters, and materials. If not explicitly stated otherwise, the summarized results have been obtained from the characterization of carbon fiber/epoxy prepreg systems which represent the standard in AFP and ATL manufacturing of large aerospace structures.[107]

4.1.1 | Temperature

Selective adjustment of temperature is the most effective and at the same time workable process-related measure to control prepreg tack.[47] Modern lay-up machines are equipped with infrared heaters or hot air guns to heat up the laminate locally before prepreg placement. Additionally, heated tools can be utilized to enhance tack to the mold or previously laid plies.[108] For industrial application, suitable temperature windows are still defined by trial-and-error approaches.[109] This may contribute to the fact that efforts have been put into the heat transfer simulation to predict temperature distribution in thermoset lay-up processes.[110–113] Although considered a matter of process parameter adjustment, control of temperature strongly governs both environmental and material influences as well. Hence, prepreg tack as a function of temperature has been targeted by several experimental studies with most of them revealing a significant correlation. Ahn et al. found a bell-shaped curve featuring a tack maximum at medium temperatures.[103] The observation has been proven consistent for peel testing by Crossley[21] and in our previous work[63] utilizing a probe test method in a rheometer (see Figure 5).

Prepreg tack is found to be very sensitive to temperature variation: For all three studies, tack rises to a maximum and falls to practically zero within the span of less than 50 K. The temperature of maximum tack deviates around room temperature most likely due to different utilized measurement methods, test parameters, tack indicators, and materials. However, a tack maximum indicates that at least two contrasting temperature-dependent mechanisms have to prevail. In all of these studies, evidence was found that for low temperatures poor tack values are achieved due to insufficient interface wetting resulting in adhesive failure between prepreg and substrate. For higher temperatures, wetting improves while the epoxy matrix is not able to provide high shear resistance during debonding due to a temperature-dependent decrease in viscosity (see Section 4.3.1 for more details). Here, matrix fibrillation and residue on the substrate can be observed which indicates cohesive failure within the bulk material. Bringing both temperature-dependent mechanisms together, maximum tack performance can be achieved in the transition region from adhesive to cohesive failure.[86,88] The adhesion-cohesion balance[114] is described as a tradeoff between providing sufficient adhesive interaction at the material-substrate interface and cohesive strength. This observation is considered a PSA fundamental[115] and seems to determine the nature of prepregs in the same matter. The adhesive properties of PSA are traditionally divided into tack, peel adhesion, and shear strength.[116–118] According to this differentiation, tack is the ability to adhere quickly, peel adhesion is the resistance against peel removal and shear strength is a measure to hold the adhesive in position when shear forces are applied.[119] The categorization appears to be reasonable when taking the adhesion-cohesion balance into consideration. For prepregs, however, this distinction has not asserted itself substantially (yet). All adhesive influences are rather combined in the term prepreg tack with very limited differentiation made.

Other studies on the temperature dependence of prepreg tack found that prepreg tack follows monotonic
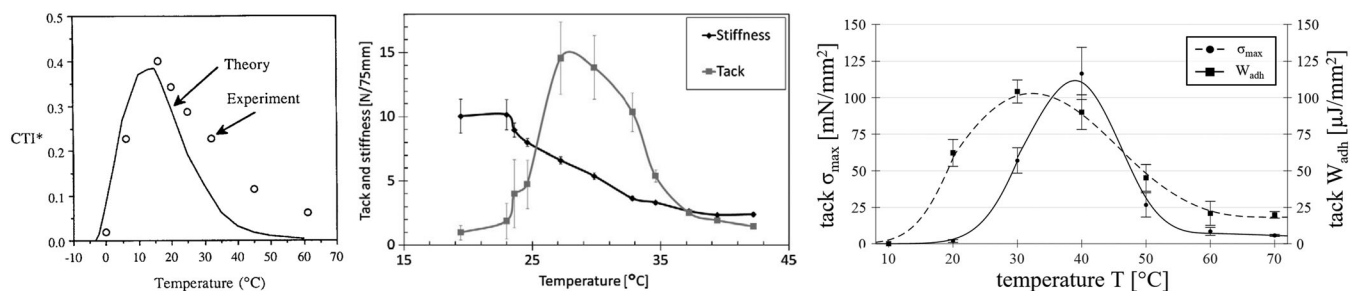

FIGURE 5 Bell-shaped curves of prepreg tack as a function of temperature. Left: reprinted from ref. [104] with permission from Wiley, 1992. Center/right: Reprinted from refs. [21] and [63] with permission from Elsevier, 2012 and 2019

functions. Putnam et al.[102] report a decrease in tack for elevated temperatures. The quantitative results from probe tack testing are correlated to a perceived qualitative rating provided by Boeing manufacturing personnel. Dubois et al.[65] found tack to exponentially decrease as a function of probe temperature within the investigated temperature range. Other studies revealed an increase in prepreg tack performance when raising the temperature.[93,94] These findings are neither contradictory to each other nor to the bell-shaped curves in Figure 5. Instead, test conditions are most likely chosen in a way that the results display one side of the bell-shaped curve. Extending the investigated temperature range would have most likely revealed a tack maximum as a result of temperature dependent improved wetting and decreased cohesive strength.

4.1.2 | Compaction force and time

The manufacturing aspects of AFP and ATL presented in Section 2 illustrate that prepreg tack depends on a sequence of both the bonding and the debonding processes. In order to achieve optimum bonding conditions, intimate contact of the prepreg material toward the substrate is crucial. Process-related factors, which determine the true contact area, are the compaction force/stress applied by the consolidation roller as well as the time of compaction also known as dwell time. Figure 6 shows tack of prepreg measured by Dubois[65] with the help of a probe test setup.

Prepreg tack is found to increase as a function of both compaction force and time. The results are supported by several studies utilizing different test methods.[16,88,104,105] Hence, the influence seems to be independent of the
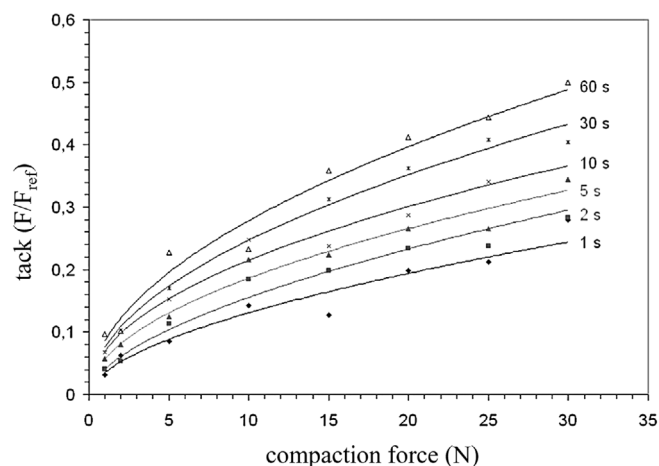

FIGURE 6 Tack as a function of compaction force and compaction time at 30°C probe temperature. Reprinted from ref. [65] with permission from Springer Nature, 2009. Figure labels were renewed for improved readability

measurement technique. Figure 6 evidently showcases that a lack of tack due to insufficient compaction force can be countervailed by an increase in dwell time. This measure, however, conflicts with a productive lay-up process as compaction time is inversely proportional to the lay-up speed in AFP and ATL processes.[120] Experimental results from some studies on compaction force and pressure are subject to restrictions in terms of manufacturing transferability. Test parameters often do not reflect lay-up conditions adequately,[84] as, for example, compaction time is limited to a few milliseconds depending on lay-up speed and compact roller dimensions.[121]

The aforementioned true contact area describes the actual area that is wetted by the adhesive or the prepreg resin respectively during the bonding process.[122–124] The concept was adapted by Gillanders[16] (probe test) and Endruweit[87] (Crossley apparatus) who both determined the true contact area of prepreg resin to glass plates after defined compaction. The results were correlated with results from tack measurement and a correlation between the true contact area and prepreg tack was found: True contact area as function of compaction force converges a maximum logarithmically indicating 100% intimate contact. Tack follows compaction force in the same way (also see Figure 6) which entails linear relationship between prepreg tack and true contact area. Consequently, maximum prepreg tack in terms of the bonding process is achieved when the substrate is fully wetted. The influence of the compaction roller (stiff vs compliant roller) on prepreg tack was also studied.[88] Differences in tack were observed and attributed to differences in pressure distribution and contact time between both rollers. The actual deformation behavior of the investigated rollers remained unknown in the study.

Although considered an intrinsic material property to be discussed in detail in Section 4.3.1, resin viscosity is crucial when discussing contact formation. Dahlquist, in this context, made a proposal on what a PSA has to fulfill in terms of flow to efficiently make contact to substrates[125]: Storage modulus G' measured by dynamic mechanical analysis (DMA) or oscillatory rheology has to be below 3×10^6 dyne/cm^2 or 0.3 MPa, respectively. Despite its simple nature, the proposal has proven to be surprisingly applicable independent of the utilized adhesive or substrate.[126,127] The validity of the Dahlquist Criterion for the viscoelastic and tack properties of prepregs was eventually tested by Crossley et al.[21] The authors found prepreg tack to generally follow the criterion's principle of improved contact for lower moduli but numerical values differ from the 0.3 MPa proposed by Dahlquist. The discrepancy is credited to prepreg-characteristic features such as fiber surface pattern and impregnation conditions discussed in Section 4.3.2.

4.1.3 | Debonding rate

The debonding rate is perceived as the velocity of material removal during prepreg-substrate separation and is highly dependent on the individual defect (Section 2.2). Instantaneous peeling of laid prepreg by the placement head will, for example, occur at much higher debonding rates (approximately at lay-up speed) than for the rather slow prepreg detachment due to bridging. The debonding rate has a significant influence on the measured stress-strain curves and, therefore, on the final tack performance as reviewed in the following.

Most of the studies which targeted the influence of debonding rate on prepreg tack found an increasing tack response when the prepreg-substrate interface is broken up at higher rates.[16,62,63,65,105] It has to be noted, however, that especially for probe testing, the shapes of the stress-strain curves change drastically when varying the debonding rate as pointed out by Dubois et al.[65] When comparing the stress-strain curves of different studies in literature, high-rate curves show a more surface-near, adhesion-controlled fracture (with little or no fibrillation) resulting in a high tack value of F_{max} and lower W_{adh}, respectively. Hence, the dependency of tack on the debonding rate is highly contingent on the used tack indicator. Böckl et al.[91] report a decrease in transverse friction force as a function of velocity. Still, the applied measurement technique differs fundamentally from peel or probe testing which may explain the discrepancy.

Observations similar to the depicted probe testing results have been made employing peel testing methods such as the Crossley apparatus: In ref. [85], an inverse logarithmic relationship between the debonding rate and temperature is reported. This has led to the suggestion that the time-temperature superposition principle (TTS) may be applicable toward prepreg tack which has been confirmed repeatedly for peel testing in subsequent studies.[21,86–88] Here, dynamic prepreg stiffness was found to increase monotonically as a function of feed rate while bell-shaped curves are determined experimentally for tack. The rate dependency of tack, for example, for PSA, has traditionally been explained based on viscoelastic behavior exhibited by polymers during the debonding process.[128] The role of prepreg resin viscosity and TTS are discussed in detail elsewhere (Section 4.3.1).

4.1.4 | Contact material

Following the prepreg material on its way through AFP or ATL heads, it makes contact to different tack-exhibiting surfaces such as the compaction roller, guiding elements, backing paper and eventually the mold or previously laid plies (see Section 2.1). Generally, most experimental studies resort to only one material which the tack of a single layer of prepreg material is measured toward. The most commonly used material combinations are prepreg-steel and prepreg-prepreg. In addition, research was conducted to selectively quantify the influence of different surface combinations. These studies yield a common result: Whenever tack between two prepreg layers was determined and compared to other material combinations, tack was found to be highest for the prepreg-prepreg combination. Endruweit et al.[88] report the adhesive performance of the prepreg-prepreg combination to be 2.5 to 5.5 higher than for prepreg-steel depending on the face. No effective tack toward fluorinated ethylene propylene representing the surface coating of the compaction roller was detected. The findings from tack measurement can serve as a quantitatively based explanation for the first-ply tack problem which estimates that a successful lay-up of the first ply on the mold as being the most difficult.[129,130] Crossley et al.[85] compared the peel tack of ATL prepreg tape toward stainless steel and composite tool with/without a mold release agent. The experimentally determined tack responses, which were rudimentarily validated by subsequently performed ATL trials, are shown in Figure 7.

A significant influence of the contact material is reported with the release agent eliminating the largest portion of prepreg tack toward the composite tool surface. In this context, Nguyen[94] performed first ply tack tests with various types of release films aiming at reliable process conditions for vertical tow placement. Differences between the release films were observed as a function of temperature. According to Figure 7, stainless steel exhibits highest tack among the investigated materials of
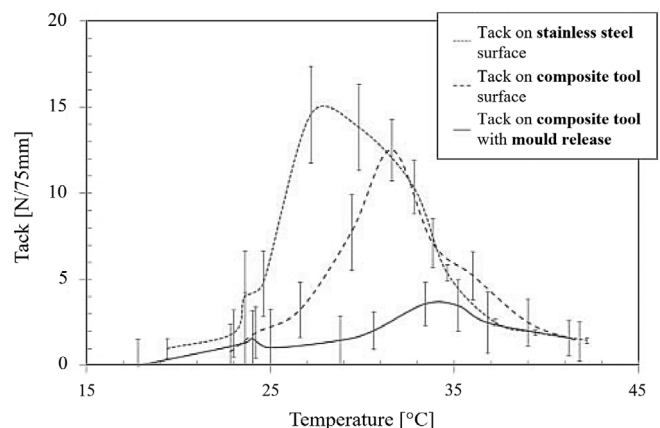

FIGURE 7 Peel tack of automated tape laying (ATL) prepreg tape toward different contact materials. Reprinted from ref. [85] with permission from Taylor & Francis, 2011. Figure labels were renewed for improved readability

the study. However, it must be noted that the prepreg-prepreg combination was not investigated at this point and tack tests on stainless steel were limited to a single level of surface roughness.[85] The latter aspect may be of importance for prepreg tack as the effect of the adherend surface roughness on the tackiness of soft adhesives has been demonstrated for PSA.[131,132] This may contribute to physical adhesion mechanisms such as mechanical interlocking.[133]

Previous considerations in combination with the influence of compaction force and dwell are the basis for the adhesive portion of bonding between prepreg resin and the substrate of interest. Interfacial interaction with the substrate is most likely caused by intermolecular forces (IMFs), namely different types of van der Waals forces and H-bonding.[134] These interactions are known to range roughly two magnitudes below covalent bonds in terms of bond energies (1-25 kJ mol^{-1} vs >200 kJ mol^{-1}[135]) which account for the low separation energies of prepreg tack compared to physically or chemically curing adhesives. Although the epoxy matrix is evidently able to chemically react (for final autoclave cure), prepreg tack is not determined by covalent bond formation toward the substrate but is rather a matter of the aforementioned IMF. The intermolecular adhesive interaction between prepreg resin and substrate has not been investigated despite its very probable crucial role. This should be encountered by further research efforts - for example, in the form of analyzing the temperature-dependent wetting behavior of different surfaces by epoxy resin using contact angle measurement. Potential results would contribute to the fundamental understanding of prepreg tack mechanisms.

4.2 | Environmental factors

The time-temperature dependent curing and moisture pickup process of prepreg material progresses primarily in the time span of ambient environment exposure between freezing and AFP/ATL processing.[136] There is an interdependency between both factors as moisture absorption by epoxy resin has been shown to accelerate the curing reaction.[137] However, for their influence on prepreg tack, both aspects have mostly been investigated independently as reviewed in the following.

4.2.1 | Ageing and DoC

The fact that targeted ageing of prepreg material is occasionally performed in industrial practice in order to control prepreg tack prior to lay-up highlights the crucial

role of this environmental factor. It is represented on data sheets in the form of tack life which indicates the time span of suitable tack properties after removal from the freezer. Thermoanalytical methods have been combined with tack measurement in order to investigate the influence of ageing-related cure behavior on prepreg tack. In their early study on the topic, Ahn et al. [103] report a temperature-dependent tack maximum which decreases for increasing storage times. Tack of fresh prepregs was compared to the adhesive properties of prepreg material which was stored at −18°C for 46 months and an additional exposure to 75°C for 3 hours, respectively. The tack maximum, however, remains constant at temperatures 20°C to 25°C above the glass transition temperature T_g shifting toward higher temperatures with increasing ageing times. The same phenomenon but for slightly different temperatures (40°C-45°C above T_g) is reported in ref. [63]. The temperature difference between both studies may be attributed to diverse ageing temperatures and times (46 months at −18°C vs 5-60 days at room temperature). The shift of maximum tack as a consequence of progressive material ageing was also substantiated by results from TTS for peel testing (see Section 4.3.1 for details) performed in ref. [88]. It was deduced from these studies that a certain flowability is necessary for surface wetting and, consequently, for a considerable tack to be measured. Matrix vitrification when tack measurement temperature is set below T_g, therefore, appears to greatly restrain surface wetting. In this case, the aged prepreg's bending stiffness increases drastically resulting in deteriorated drape. This issue is reflected in Figure 8 which shows the ageing-related evolution of DoC and T_g for a carbon fiber/epoxy prepreg measured by differential scanning calorimetry.

DoC and T_g rise steeply within the first 10 days (tack life) with T_g reaching room temperature after this time span. Tack measured at room temperature for 10 days'
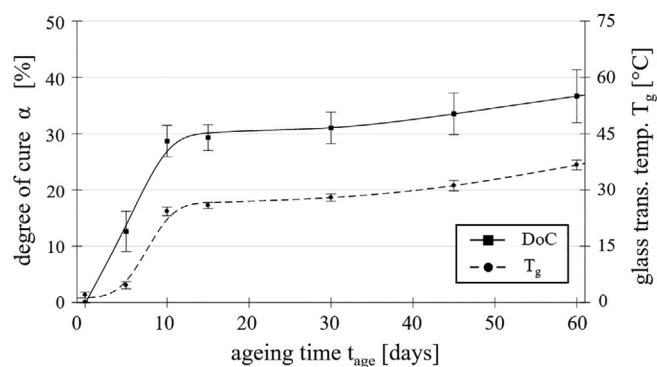

FIGURE 8 Effect of room temperature ageing on kinetic properties of carbon fiber/epoxy prepregs. Reprinted from ref. [63] with permission from Elsevier, 2019

—WILEY | **3451**

old prepreg was completely lost, while an increased work of adhesion (up to 66%) was measured at elevated temperatures. The bell-shaped curves described by Ahn et al.[103] were found to be shifting toward higher temperatures as prepreg resin viscosity increases in the wake of progressing cure reaction.[63] This assumption of ageing-affected molecular mobility can serve as an explanation for the somewhat contradictory results that are reported for the dependency of prepreg tack on ageing: While a decrease in tack was measured in refs. [65], [88], [91], and [106], a (temperature-related) increase is observed in refs. [63] and [93].

Several attempts have been made in literature to produce prepregs on laboratory-scale prepregging machines with tailored processing-relevant properties including tack. Tack properties were adjusted by the selective control of the level of resin cure (B-staging). The DoC of commercial prepregs in B-stage is known to be 25% to 35%.[138] Banks et al.,[98] who developed a structural glass/epoxy prepreg for marine and civil infrastructure applications, report maximum fracture energy at 30% DoC (Figure 9).

The value was also specified as the optimum level of resin cure in the tradeoff between handling, drape, and tack. Tack maxima as a function of DoC were also reported by Rajaei[96] and Shaghaghi[97] who investigated tack of phenolic/glass prepregs. However, tack maximum of phenolic prepregs formed at significantly lower conversion of 5.3% precure compared to epoxy-based systems.[96] Novolak and resole types of phenolic resins were shown to exhibit varying tack levels.[97] A direct comparison between epoxy and phenolic prepregs with different types of fiber reinforcements was drawn by Smith et al.[64] Even carbon fiber prepregs with

thermoplastic matrices that usually do not exhibit any tack at all near ambient temperature have been investigated for their levels of tack most recently: Shin et al.[139] performed tack tests on lab-scale produced prepregs using carbon fiber fabric and partially polymerized poly(methyl methacrylate). Tack decreased rapidly as a function of ageing-induced polymerization and was completely lost after 60 minutes of ambient exposure.

4.2.2 | Moisture

Apart from tack implication, moisture absorption in uncured prepregs may result in void formation in out-of-autoclave laminates[140,141] and to a lesser degree even in autoclave-cured composite parts.[142] Water in the form of sorbed moisture is known to plasticize epoxy resins[143] affecting the processability of prepregs in the same manner as the mechanical performance of cured parts. Buehler and Seferis[99] studied water absorption and desorption of glass and carbon fiber prepregs and conducted tack measurement on these materials with low and high solvent contents (from impregnation process). While water uptake was found to peak at 11% to 13% after 1200 hours of absorption, moisture drops to 3% after 450 hours of additional exposure in a desorption environment. No tack results are presented for the moisture exposed specimens but the adhesive properties of glass prepreg are reported to have doubled after solvent removal. Wohl et al.[62] investigated the combined impact on tack which is entailed by changes in relative humidity conditioning in combination with other input parameters (contact time, contact force, and temperature). The surface plots from probe tack testing using a rheometer as a test apparatus are displayed in Figure 10.

Together with the other displayed input variables, a parameter set could be determined by optimization analysis in order to achieve maximized F_{adh}. Desirability for maximum tack includes relatively low temperature, high contact time and a specific threshold of compaction force. For humidity, however, interdependencies with other input variables turn out to be more complex as moderate to high values should be favored.[62]

The partly ambiguous dependence of tack on water uptake can be seen in the peel test results performed in ref. [88]. Here, lower tack values in general are reported for humidity-exposed samples (33%, 43%, and 59% RH) than for unconditioned prepregs on the one hand. This finding was also made by Dubois for 80% and 20% RH exposure.[65] On the other hand, a significant increase in tack from 34% and 43% to 59% RH is observed in ref. [88] which appears to be contradictory considering the generally lower tack of conditioned specimens compared to
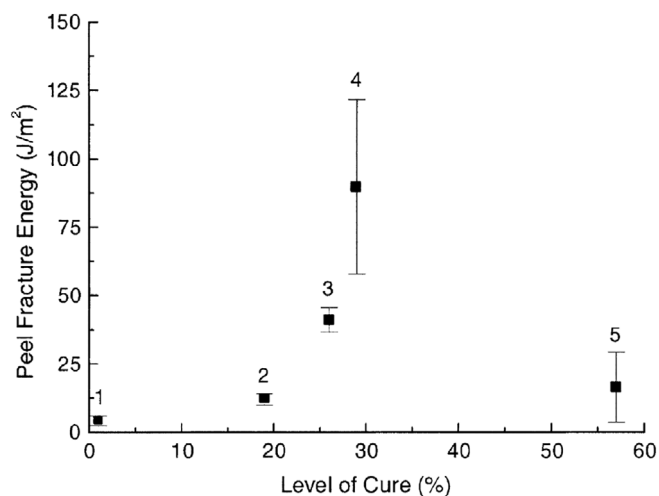

FIGURE 9 Prepreg tack as a function of cure level. Reprinted from ref. [98] with permission from Elsevier, 2004
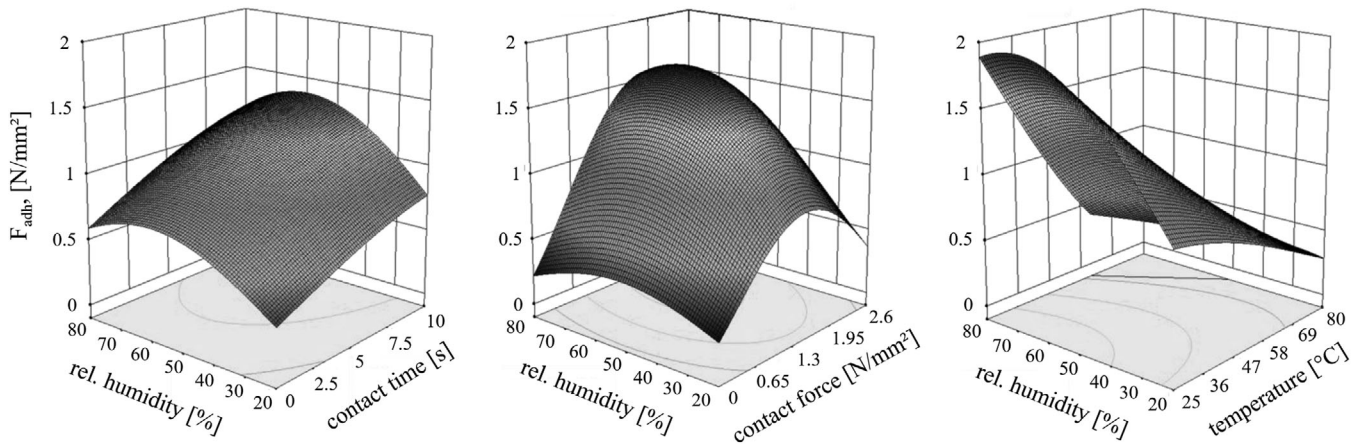
FIGURE 10 Response surfaces of tack (F_{adh}) measured as a function of relative humidity and second input variables (contact time, contact, and temperature). Reprinted from ref. [62] with permission from the Society for the Advancement of Material and Process Engineering (SAMPE), 2017. Figure was rearranged and labels renewed for improved readability

fresh prepreg. The authors consider plasticization effects to be responsible for this. In summary, the small number of studies on the topic has revealed that there is a significant influence on humidity exposure and accompanied moisture uptake on prepreg tack. Still, causal relationships are not fully understood yet and require further studying.

4.3 | Material properties

Prepregs for automated lay-up technology are commercially available in a wide range of material properties, for example, in terms of matrix formulation, fiber type, and reinforcement weight. As a result, composite manufacturers can opt for material systems meeting their demands for both the final part performance as well as the processing factors including tack.

4.3.1 | Resin viscosity

Prepreg matrix resins and PSA traditionally differ in terms of polymer formulation. While epoxies, cyanate esters, and phenolic resins are mainly used for prepreg material, a large variety of both natural and synthetic polymers such as acrylics,[144–146] natural rubbers,[147] polyurethanes,[148] polyvinyl ethers,[149] and many more, are processed for PSA. Despite the difference, both materials are based on polymers and, therefore, exhibit viscoelastic behavior which decisively affects their tack properties. Time, shear rate, and temperature dependence of prepreg resin viscosity has thus been analyzed in several studies and brought together with tack characterization as reviewed below.
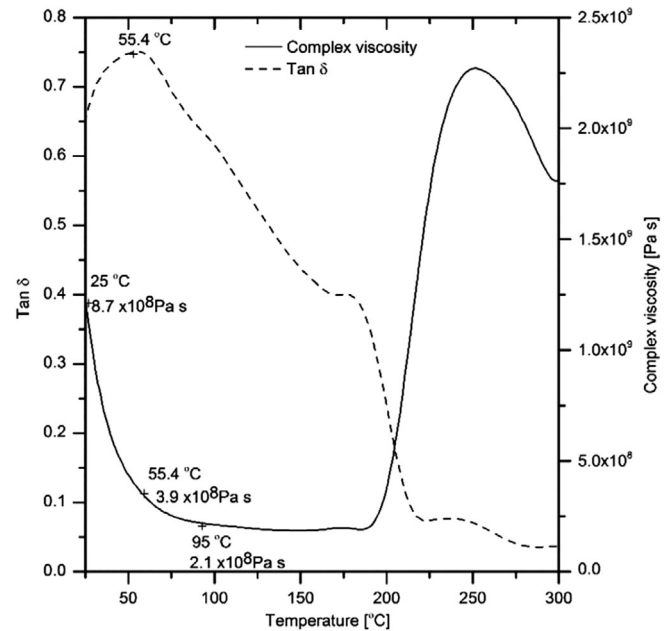

FIGURE 11 Loss factor tan δ and complex viscosity of epoxy towpreg resin as a function of temperature (1 Hz, 5 K min^{-1}). Reprinted from ref. [95] with permission from SAGE, 2016

In order to exhibit maximum tack, prepreg resin viscosity needs to fulfill contradictory requirements in agreement with the temperature discussion in Section 4.1.1: good viscous flow for substrate surface wetting and high viscosity for a certain shear resistance during debonding ([98,150]; also see Dahlquist's criterion in Section 4.1.2). The first aspect was targeted by Rao et al.[95] who set up a full factorial DOE for lay-up load, speed, and temperature. Peel tack was recorded as a function of input parameters and additional DMA was conducted for viscoelastic characterization. Figure 11 shows the

—WILEY—

complex viscosity and loss factor tan δ in a temperature range between room temperature and 300°C.

The authors report a strong increase in peel force for both input parameters compaction load and speed when raising the temperature from 25°C to 65°C. Within the investigated temperature range, complex viscosity drops by almost a full magnitude from 1.25 to 0.2×10^9 Pa s. Tan δ, which describes the ratio between loss modulus G'' (viscous portion) and storage modulus G' (elastic portion), following accordingly from 0.4 to 0.1 indicating a strong shift toward a more viscous behavior of the matrix resin. The rheological findings were considered to be responsible for improved surface wetting and, consequently, a higher measured tack. However, the debonding process was not taken into consideration. Both viscosity and the cohesive debonding portion of tack were shown to follow Arrhenius-type, exponentially decreasing functions of temperature elsewhere.[63]

Ahn et al.[104] used the resin viscosity as one of four intrinsic material parameters to describe prepreg tack as a bulk viscoelastic property and developed a model presented in Section 5. The correlation between matrix viscosity and tack can also be represented by the TTS principle. With the help of the concept, polymer viscoelasticity is described over a wide range of deformation rate and temperature.[151] It allows master curves to be produced based on shift factors from models such as the William-Landel-Ferry equation[152] or Arrhenius plots.[123,124] For PSA, the applicability of the principle to tack was demonstrated early by Kaelble in the 1960s[153] and frequently reproduced in PSA research.[54,154] Crossley[86] successfully transferred TTS to prepreg tack (and dynamic stiffness) with the help of the WLF equation and experimental data from oscillatory rheology and peel tack measurement. Figure 12 shows the shifted tack curves of a glass/epoxy ATL tape as a function of feed rate V (debonding rate) and temperature.

A high degree of overlapping shifted tack curves for different temperatures indicates the general applicability of the principle to prepreg tack. Surprisingly, it was found that the TTS relationship could be employed for both adhesive and cohesive prepreg fracture, in other words, the left and the right slopes of the bell-shaped curves. Usually for PSA, only cohesive failure within the adhesive follows the TTS principle (see PSA references above). A discussion on this topic for prepregs can be found at the end of ref. [86] as well as in other studies by the authors,[21,87,88] in which the TTS concept was repeatedly reapplied for further investigation.

In the context of viscosity and tack, Chang developed the Chang Window[155] which classifies PSAs into different specialist applications (protective films, medical tapes, labels, etc.) as a function of complex rheological data, namely G' and G'' measured at different
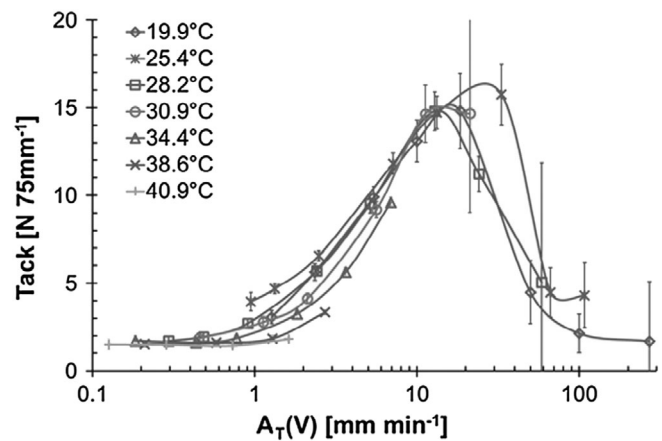

FIGURE 12 Tack curves shifted by time-temperature superposition. Reprinted from ref. [86] with permission from Elsevier, 2013

frequencies. The window's deformation frequency range ($\approx$ tack measurement range) was set to 0.01 to 100 s^{-1} by Chang. Direct transfer of prepreg tack data toward the Chang Window has not been performed yet despite its active reception in PSA research.[114] However, a similar categorization for prepregs can be beneficial if viscoelastic classification is possible, for example, according to data sheet information (low, medium, high tack) or even its matter of use (AFP/ATL/hand-layup).

4.3.2 | Prepreg architecture and fiber volume fraction

The presence of reinforcement fibers in prepregs is the most apparent distinctive feature in comparison to the homogeneous, bulk-like appearance of PSA layers. Investigating the role reinforcement fibers on the adhesive performance of prepreg, therefore, is essential. Crucial aspects are the fiber volume fraction (FVF) as well as the local distribution of both prepreg components.

In ref. [65], stress-strain curves obtained from probe testing pure epoxy "pancakes" and prepreg were compared and discussed. The authors attribute differences in the shape of single displacement phases (cavitation, fibrillation, etc.) to the presence of reinforcement fibers in the prepreg material. The structural aspects discussed are gradients of resin content in z-direction, prepreg roughness due to surface-near fibers and others. Endruweit et al.[87,88] investigated the tack of the inner (when on a roll; no protective paper: "N-Face") and outer (with paper: "P-Face") face of ATL tape. Experimental data revealed a 93% higher peel tack of the P-Face toward steel than for the N-Face. The difference was attributed to different distributions and volume of resin on the surface. However,

very little discrepancy was found between P-P and N-N prepreg-prepreg combinations. It was generally deducted that prepreg architecture influences both adhesive and cohesive mechanisms of prepreg tack. In the same studies, a sharp rise in tack was measured for larger inter-ply angles between two prepreg layers. Peel tack increases by 67% from 0° to 90° ply angle.

Hayes et al.[101] produced prepregs from UD carbon fibers and a model epoxy resin formulation in order to investigate the influence of hotmelt prepregging-related structural properties on prepreg tack. As a result, the impregnation parameters (pressure and temperature) were varied and prepregs were examined in terms of impregnation level and FVF. The results from probe tack testing are displayed in Figure 13.

Increasing both impregnation parameters leads to a better impregnation level and a slightly raised FVF.

Considering this anticipated relationship, it can be concluded from Figure 13 that the higher the impregnation level of the prepreg is, the lower the measured tack will be. The correlation was attributed to an insufficient amount of surface resin to fully wet the interface. In contrast, a thicker bulk resin layer will contribute to the viscoelastic debonding if the prepreg is poorly impregnated. This finding supports the industrial prepregging practice of impregnating reinforcement fibers partly or adding a second tack-enhancing layer.[47]

5 | MODEL APPROACHES

Model approaches to tack of prepregs have rarely been presented in literature compared to the numerous and partially elaborate models developed for PSA.[156–158]
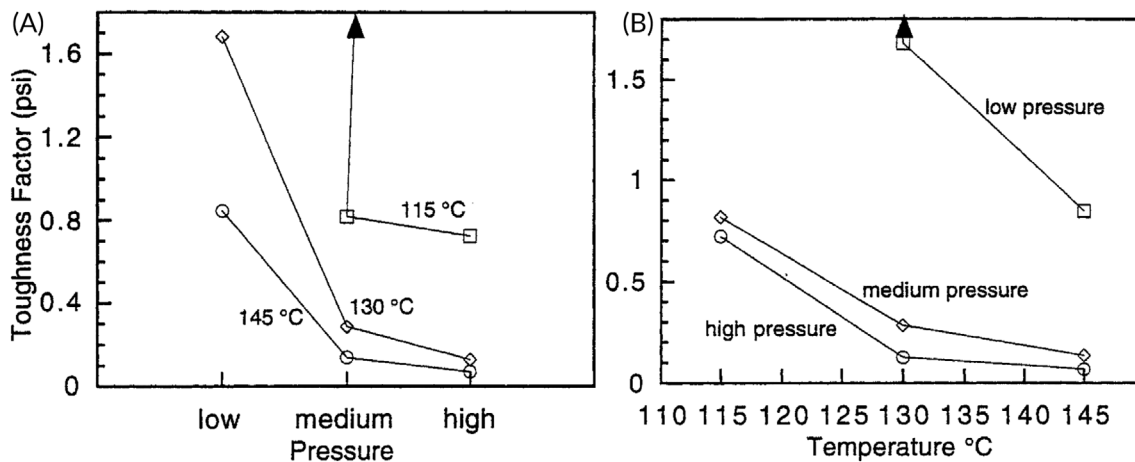

FIGURE 13 Tack (toughness factor) as a function of impregnation pressure and impregnation temperature. Reprinted from ref. [101] with permission from Wiley, 2004
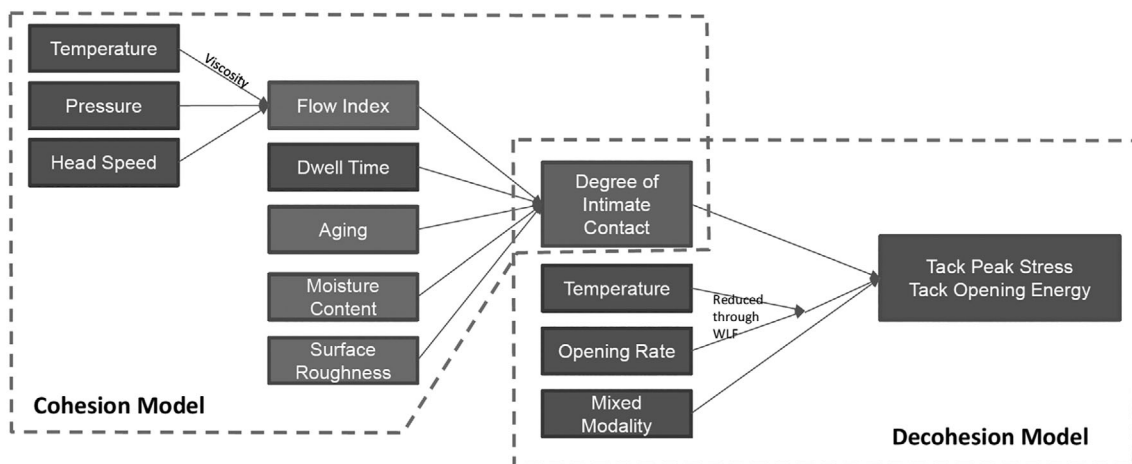

FIGURE 14 Flowchart presenting dependencies on tack response. Reprinted from ref. [159] with permission from the Society for the Advancement of Material and Process Engineering (SAMPE), 2017

Research on prepregs has focused on utilizing experimental methods for characterization instead, as presented in the previous chapter. In 2011, Lukaszewicz[120] stated that "tack is still a prepreg property that is not fully explored and cannot be accounted for in process models." Almost a decade later, the first claim of his statement has been alleviated by continuing research but in our opinion still holds in general. However, knowledge on prepreg tack has reached a state of basic model applicableness as recently demonstrated by Forghani et al. who have presented a modeling framework for the simulation of prepreg tack in AFP processes.[159,160] The proposed numerical tack model ([161]; Figure 14) is based on experimental calibration by probe tack testing in a rheometer as presented in ref. [62].

Tack phenomena are split into two stages, namely, the cohesion and decohesion stages, which represent influencing factors of the bonding/compaction and the debonding/separation phases. Both stages are modeled separately with the so-called degree of intimate contact (DoIC, ratio of wetted contact area) acting as the linking intermediate state variable ($0 \leq \text{DoIC} \leq 1$). A validation study[162] in the model framework was eventually conducted that aimed at demonstrating the model's ability to predict defect formation in AFP steering for a simple curve arc.

Ahn et al. present an early attempt to describe prepreg tack as a bulk viscoelastic property of a laminate stack.[104] The authors used the standard linear solid model, which had been proven applicable for thermoset composite materials before,[163,164] and modified it with regard to prepregs (void content, fiber areal weight, etc.). Four intrinsic material parameters from viscoelastic analysis were determined and represented in the model. Good agreement between model prediction and experimental data was found. Experimental data include the stress-strain curves from probe tack testing and the tack indicator called compression tack index (CTI*) which is defined as the ratio of output energy while debonding and the compressive input energy during bonding. Some authors of later experimental studies on prepreg tack reuse the CTI* as a tack indicator.[63,100]

6 | CONCLUSION/FUTURE PERSPECTIVE

This review article presents a summary and discussion of the current state of research on the adhesive behavior of prepreg material and its relevance for automated lay-up technology. The characterization of prepreg tack has been an active area of research for several decades and was shown to be primarily targeted by employing experimental methods of investigation in the past. The lack of a standardized measurement technique has led to different methods of quantifying the tack of thermoset preimpregnated fiber composite fibers. The variety of measurement techniques employed in combination with a large set of tack-determining influence parameters makes it difficult to describe the complex mechanisms of prepreg tack thoroughly. Consequently, misinterpretation of experimental results may occur easily when investigating single parameters within narrow variation intervals. Seemingly contradictory results, however, can be explained by the adhesion-cohesion balance as demonstrated repeatedly throughout this review article. It can be regarded as a prepreg tack fundamental representing the tack-governing mechanisms of intimate contact formation and viscoelastic deformation behavior. Generally, the instantaneous adhesion upon the light pressure application of prepregs resembles the behavior of PSA. The profound knowledge base of longtime research on PSA has been steering and will continue to steer prepreg tack characterization in the future by providing proven experimental, modeling and simulation approaches.

Although considerable knowledge on prepreg tack has been generated by experimental investigation and has yielded first process modeling approaches to this day, substantial shifts toward selective process adjustment have not yet been made. However, this will be the next step necessary to overcome the trial and error-based practice in AFP and ATL. Validation studies are necessary in order to prove that tack measurement and model results can be turned into successful operating points of composite manufacturing systems. This way, prospective process improvement can be achieved by increased robustness toward laminate defects and machine breakdown. Challenges will arise when conciliating measures of tack-relevant process adjustment and production efficiency, for example, in terms of lay-up speed or material storage.

ACKNOWLEDGMENTS

ORCID
Dennis Budelmann https://orcid.org/0000-0003-4465-5714

REFERENCES
[1] E. S. Nelson, D. R. Reddy, *Green Aviation: Reduction of Environmental Impact through Aircraft Technology and Alternative Fuels*, CRC Press, Boca Raton, FL **2018**.

[2] T. Siddiqui, *Aircraft Materials and Analysis*, McGraw-Hill Education, New York, NY **2015**.

[3] J. Frketic, T. Dickens, S. Ramakrishnan, *Addit. Manuf.* **2017**, *14*, 69.

[4] P. K. Bajpai, I. Singh, *Reinforced Polymer Composites: Processing, Characterization and Post Life Cycle Assessment*, Wiley VCH, Weinheim, Germany **2019**.

[5] M. Jawaid, M. Thariq, *Sustainable Composites for Aerospace Applications*, Elsevier, Cambridge **2018**.

[6] F. C. Campbell, *Manufacturing Technology for Aerospace Structural Materials*, Elsevier Science, Amsterdam, the Netherlands **2011**.

[7] M. N. Grimshaw, C. G. Grant, J. M. L. Diaz, SAMPE 2001, Long Beach, CA **2001**.

[8] C. Grant, *Ind. Robot* **2006**, *33*, 117.

[9] K. A. Jeffries, *SAE Int. J. Aerosp.* **2013**, *6*, 774.

[10] Y.-N. Liu, C. Yuan, C. Liu, J. Pan, Q. Dong, *Sci. Rep.* **2019**, *9* (1), 7440.

[11] R. P. Smith, Z. Qureshi, R. J. Scaife, H. M. El-Dessouky, *J. Reinf. Plast. Compos.* **2016**, *35*, 1527.

[12] G. Marsh, *Reinf. Plast.* **2011**, *55*, 32.

[13] I. Benedek, *Developments in Pressure-Sensitive Products*, CRC Press, Boca Raton, FL **2005**.

[14] S. Ebnesajjad, A. H. Landrock, *Adhesives Technology Handbook*, Elsevier Science, Amsterdam, the Netherlands **2014**.

[15] W. Brockmann, P. Ludwig Geiß, J. Klingenberg, B. Schröder, *Adhesive Bonding*, Wiley-VCH, Weinheim, Germany **2009**.

[16] A. M. Gillanders, S. Kerr, T. J. Martin, *Int. J. Adhes. Adhes.* **1981**, *1*, 125.

[17] K. L. Stone, SAMPE 1984, Reno, NV **1984**.

[18] H. L. Eaton, SAMPE 1984, Reno, NV **1984**.

[19] R. A. Meier, SAMPE 1986, Covina, CA **1986**.

[20] D. H.-J. A. Lukaszewicz, C. Ward, K. D. Potter, *Compos. Part B* **2012**, *43*, 997.

[21] R. J. Crossley, P. J. Schubel, N. A. Warrior, *Compos. Part A* **2012**, *43*, 423.

[22] B. Denkena, C. Schmidt, K. Völtzer, T. Hocke, *Compos. Part B* **2016**, *97*, 239.

[23] T. R. Brooks, J. R. R. A. Martins, *Compos. Struct.* **2018**, *204*, 548.

[24] F. Shadmehri, O. Ioachim, O. Pahud, J. E. Brunel, A. Landry, S. V. Hoa, M. Hojjati, *20th Int. Conf. on Composite Materials*, Copenhagen, DK **2015**.

[25] J. P.-H. Belnoue, T. Mesogitis, O. J. Nixon-Pearson, J. Kratz, D. S. Ivanov, I. K. Partridge, K. D. Potter, S. R. Hallett, *Compos. Part A* **2017**, *102*, 196.

[26] X. Li, S. R. Hallett, M. R. Wisnom, *Sci. Eng. Compos. Mater.* **2015**, *22*, 115.

[27] T. J. Dodwell, R. Butler, G. W. Hunt, *Compos. Sci. Technol.* **2014**, *105*, 151.

[28] J. Brüning, B. Denkena, M.-A. Dittrich, T. Hocke, *Proc. CIRP* **2017**, *66*, 74.

[29] K. Croft, L. Lessard, D. Pasini, M. Hojjati, J. Chen, A. Yousefpour, *Compos. Part A* **2011**, *42*, 484.

[30] M. H. Nguyen, A. A. Vijayachandran, P. Davidson, D. Call, D. Lee, A. M. Waas, AIAA Scitech 2019 Forum, San Diego, CA **2019**.

[31] O. Falcó, J. A. Mayugo, C. S. Lopes, N. Gascons, J. Costa, *Compos. Part A* **2014**, *63*, 21.

[32] W. Woigk, S. R. Hallett, M. I. Jones, M. Kuhtz, A. Hornig, M. Gude, *Compos. Struct.* **2018**, *201*, 1004.

[33] A. Sawicki, P. Minguett, 39th AIAA/ASME/ASCE/AHS/ASC Structures, Structural Dynamics, and Materials Conference and Exhibit, Long Beach, CA **1998**.

[34] M. Y. Matveev, P. J. Schubel, A. C. Long, I. A. Jones, *Compos. Part A* **2016**, *90*, 451.

[35] N. Bakhshi, M. Hojjati, *Compos. Part B* **2019**, *165*, 586.

[36] N. Bakhshi, M. Hojjati, *Compos. Part A* **2018**, *113*, 122.

[37] J. Chen, T. Chen-Keat, M. Hojjati, A. J. Vallee, M.-A. Octeau, A. Yousefpour, *Sci. Eng. Compos. Mater.* **2015**, *22*, 165.

[38] C. Zhao, J. Xiao, W. Huang, X. Huang, S. Gu, *J. Reinf. Plast. Compos.* **2016**, *35*, 1576.

[39] R. Lichtinger, J. Lacalle, R. Hinterhölzl, U. Beier, K. Drechsler, *Sci. Eng. Compos. Mater.* **2015**, *22*, 131.

[40] R. Lichtinger, T. Tang, K. Drechsler, ECCOMAS 2012, Vienna, AT **2012**.

[41] D. Maass, *Reinf. Plast.* **2015**, *59*, 242.

[42] G. Nilakantan, S. Nutt, *J. Compos. Mater.* **2018**, *52*, 341.

[43] T. Oldani, SAE Aerospace Manufacturing and Automated Fastening Conference and Exhibition, North Charleston, SC **2008**.

[44] M. K. Hagnell, M. Åkermo, *Compos. Part B* **2015**, *792*, 54.

[45] P. J. Schubel, *Compos. Part B* **2012**, *43*, 953.

[46] A. Mills, *Compos. Part A* **2001**, *32*, 955.

[47] H. Lengsfeld, F. Wolff-Fabris, J. Krämer, J. Lacalle, V. Altstädt, *Composite Technology: Prepregs and Monolithic Part Fabrication Technologies*, Carl Hanser, Munich, Germany **2015**.

[48] I. K. Mohammed, M. N. Charalambides, A. J. Kinloch, *J. Non-Newtonian Fluid Mech.* **2015**, *222*, 141.

[49] ASTM D2979-16, *Test Method for Pressure-Sensitive Tack of Adhesives Using an Inverted Probe Machine*, ASTM International, West Conshohocken, PA **2016**.

[50] J. Kajtna, M. Krajnc, *Int. J. Adhes. Adhes.* **2011**, *31*, 29.

[51] M. Fujita, M. Kajiyama, A. Takemura, H. Ono, H. Mizumachi, S. Hayashi, *J. Appl. Polym. Sci.* **1998**, *70*, 771.

[52] B.-J. Kim, S.-E. Kim, H.-S. Do, S. Kim, H.-J. Kim, *Int. J. Adhes. Adhes.* **2007**, *27*, 102.

[53] P. L. Drzal, K. R. Shull, *J. Adhes.* **2005**, *81*, 397.

[54] A. Zosel, *Colloid Polym. Sci.* **1985**, *263*, 541.

[55] H. Lakrout, P. Sergot, C. Creton, *J. Adhes.* **1999**, *69*, 307.

[56] T. Yamaguchi, M. Doi, *Eur. Phys. J. E* **2006**, *21*, 331.

[57] Y. Nakamura, K. Imamura, K. Yamamura, S. Fujii, Y. Urahama, *J. Adhes. Sci. Technol.* **2013**, *27*, 1951.

[58] F. H. Hammond, *Adhesion*, ASTM International, West Conshohocken, PA **1964**.

[59] C. Creton, J. Hooker, K. R. Shull, *Langmuir* **2001**, *17*, 4948.

[60] H.-J. Kim, S. Hayashi, H. Mizumachi, *J. Appl. Polym. Sci* **1998**, *69*, 581.

[61] D. A. Dillard, A. V. Pocius, *The Mechanics of Adhesion*, Elsevier Science, Amsterdam, the Netherlands **2002**.

[62] C. Wohl, F. Palmieri, A. Forghani, C. Wade Hickmott, H. Bedayat, B. Coxon, A. Poursartip, B. Grimsley, CAMX 2017, Orlando, FL **2017**.

[63] D. Budelmann, H. Detampel, C. Schmidt, D. Meiners, *Compos. Part A* **2019**, *117*, 308.

[64] E. J. Smith, C. Grubb, J. Misasi, N. Larson, CAMX 2019, Anaheim, CA **2019**.

[65] O. Dubois, J.-B. le Cam, A. Béakou, *Exp. Mech.* **2010**, *50*, 599.

[66] Y. Peykova, S. Guriyanova, O. V. Lebedeva, A. Diethert, P. Müller-Buschbaum, N. Willenbacher, *Int. J. Adhes. Adhes.* **2010**, *30*, 245.

[67] L. F. M. da Silva, D. A. Dillard, B. Blackman, R. D. Adams, *Testing Adhesive Joints: Best Practices*, Weinheim, Germany, Wiley VCH **2012**.

[68] ASTM D6862-11, *Test Method for 90 Degree Peel Resistance of Adhesives*, ASTM International, West Conshohocken, PA **2016**.

[69] ASTM D903-98, *Test Method for Peel or Stripping Strength of Adhesive Bonds*, ASTM International, West Conshohocken, PA **2017**.

[70] ASTM D1876-08, *Test Method for Peel Resistance of Adhesives (T-Peel Test)*, ASTM International, West Conshohocken, PA **2015**.

[71] ASTM D3167-10, *Test Method for Floating Roller Peel Resistance of Adhesives*, ASTM International, West Conshohocken, PA **2017**.

[72] ASTM D1781-98, *Test Method for Climbing Drum Peel for Adhesives*, ASTM International, West Conshohocken, PA **2012**.

[73] ASTM D3330/D3330M-04, *Test Method for Peel Adhesion of Pressure-Sensitive Tape*, ASTM International, West Conshohocken, PA **2018**.

[74] D. W. Aubrey, G. N. Welding, T. Wong, *J. Appl. Polym. Sci.* **1969**, *13*, 2193.

[75] M. Sherriff, R. W. Knibbs, P. G. Langley, *J. Appl. Polym. Sci.* **1973**, *17*, 3423.

[76] N. Nakajima, R. Babrowicz, E. R. Harrell, *J. Appl. Polym. Sci.* **1992**, *44*, 1437.

[77] L. Benyahia, C. Verdier, J.-M. Piau, *J. Adhes.* **1997**, *62*, 45.

[78] ASTM D6195-03, *Test Methods for Loop Tack*, ASTM International, West Conshohocken, PA **2019**.

[79] ASTM D3121-17, *Test Method for Tack of Pressure-Sensitive Adhesives by Rolling Ball*, ASTM International, West Conshohocken, PA **2017**.

[80] A. Kowalski, Z. Czech, *Int. J. Adhes. Adhes.* **2015**, *60*, 9.

[81] Y. Woo, R. H. Plaut, D. A. Dillard, S. L. Coulthard, *J. Adhes.* **2004**, *80*, 203.

[82] H. Mizumachi, T. Saito, *J. Adhes.* **1986**, *20*, 83.

[83] R. Petersen, E. Link, Z. Miyagi, N. Yamada, N. Urahama, K. Yamamoto, *J. Test. Eval.* **1997**, *25*, 23.

[84] R. J. Crossley, P. J. Schubel, N. A. Warrior. *Proc. 17th Int. Conf. on Composite Materials*, Edingbourgh, UK **2009**.

[85] R. J. Crossley, P. J. Schubel, N. A. Warrior, *Plast. Rubber Compos.* **2011**, *40*, 363.

[86] R. J. Crossley, P. J. Schubel, D. S. A. de Focatiis, *Compos. Part A* **2013**, *52*, 126.

[87] A. Endruweit, D.S.A. de Focatiis, N. A. Warrior, S. Ghose, B. A. Johnson, D. R. Younkin, SAMPE 2016, Long Beach, CA **2016**.

[88] A. Endruweit, G. Y. H. Choong, S. Ghose, B. A. Johnson, D. R. Younkin, N. A. Warrior, D. S. A. de Focatiis, *Compos. Part A* **2018**, *114*, 295.

[89] R. J. Crossley, PhD Thesis, University of Nottingham, (Nottingham, UK) **2011**.

[90] B. Böckl, C. Jetten, K. Heller, C. Ebel, K. Drechsler, 29th SICOMP, Lulea, SE **2018**.

[91] B. Böckl, C. Jetten, K. Heller, C. Ebel, K. Drechsler, ECCM18, Athens, GR **2018**.

[92] ASTM D1002-10, *Test Method for Apparent Shear Strength of Single-Lap-Joint Adhesively Bonded Metal Specimens by Tension Loading (Metal-to-Metal)*, ASTM International, West Conshohocken, PA **2019**.

[93] D. C. Nguyen, C. Krombholz, ECCM17, Munich, Germany **2016**.

[94] D. C. Nguyen, D. Delisle, SAMPE Europe, Stuttgart, DE **2017**.

[95] S. Rao, R. Umer, J. Thomas, W. J. Cantwell, *J. Reinf. Plast. Compos.* **2016**, *35*, 275.

[96] M. Rajaei, M. Hosain Beheshty, M. Hayaty, *Polym. Polym. Compos.* **2011**, *19*, 789.

[97] S. Shaghaghi, M. Hosain Beheshty, H. Rahimi, *Iran. Polym. J.* **2011**, *20*, 969.

[98] R. Banks, A. P. Mouritz, S. John, F. Coman, R. Paton, *Compos. Struct.* **2004**, *66*, 169.

[99] F. U. Buehler, J. C. Seferis, *Compos. Part A* **2000**, *31*, 741.

[100] A. Popp, D. Klostermann, R. Chartoff, SAMPE 2000, Long Beach, CA **2000**.

[101] B. S. Hayes, J. C. Seferis, J. S. Chen, *Polym. Compos.* **1996**, *17*, 730.

[102] J. W. Putnam, J. C. Seferis, T. Pelton, M. Wilhelm, *Sci. Eng. Compos. Mater.* **1995**, *4*, 55.

[103] K. J. Ahn, L. Peterson, J. C. Seferis, D. Nowacki, H. G. Zachmann, *J. Appl. Polym. Sci.* **1992**, *45*, 399.

[104] K. J. Ahn, J. C. Seferis, T. Pelton, M. Wilhelm, *Polym. Compos.* **1992**, *13*, 197.

[105] K. J. Ahn, J. C. Seferis, T. Pelton, M. Wilhelm, *SAMPE Quater.* **1992**, *23*, 54.

[106] K. C. Cole, D. Noël, J.-J. Hechler, P. Cielo, J.-C. Krapez, A. Chouliotis, K. C. Overbury, *Polym. Compos.* **1991**, *12*, 203.

[107] A. McIhhagger, E. Archer, R. McIlhager, *Manufacturing Processes for Composite Materials and Components for Aerospace Application*, Elsevier Science, Amsterdam, the Netherlands **2015**.

[108] B. T. Astrom, *Manufacturing of Polymer Composites*, CRC Press, Boca Raton, FL **2018**.

[109] R. Lichtinger, P. Hörmann, D. Stelzl, R. Hinterhölzl, *Compos. Part A* **2015**, *68*, 387.

[110] P. Hörmann, D. Stelzl, R. Lichtinger, S. van Nieuwenhove, G. Mazón Carro, K. Drechsler, *Compos. Part A* **2014**, *67*, 282.

[111] N. Hassan, J. E. Thompson, R. C. Batra, A. Bruce Hulcher, X. Song, A. C. Loos, *J. Reinf. Plast. Compos.* **2005**, *24*, 869.

[112] T. Orth, M. Krahl, P. Parlevliet, N. Modler, *Adv. Manuf. Polym. Compos. Sci.* **2018**, *4*, 73.

[113] H. Sarrazin, G. S. Springer, *J. Compos. Mater.* **1995**, *29*, 1908.

[114] I. Benedek, *Pressure-Sensitive Adhesives and Applications*, CRC Press, Boca Raton, FL **2004**.

[115] I. Benedek, M. M. Feldstein, *Fundamentals of Pressure Sensitivity*, CRC Press, Boca Raton, FL **2009**.

[116] Z. Czech, A. Kowalczyk, in *Wide Spectra of Quality Control* (Ed: I. Akyar), InTech Open, London **2011**, p. 309.

[117] C. W. Paul, in *Handbook of Adhesion Technology* (Eds: L. F. M. da Silva, A. Öchsner, R. D. Adams), Springer, Berlin, Germany **2018**, p. 341.

[118] S. Sun, M. Li, A. Liu, *Int. J. Adhes. Adhes.* **2013**, *41*, 98.

[119] D. Satas, *Handbook of Pressure Sensitive Adhesive Technology*, Springer, New York, NY **1989**.

[120] D. H.-J. A. Lukaszewicz, PhD Thesis, University of Bristol, (Bristol, UK) **2011**.

[121] J. Cheng, D. Zhao, K. Liu, Y. Wang, H. Chen, *J. Reinf. Plast. Compos.* **2018**, *37*, 1418.

[122] C. Creton, L. Leibler, *J. Polym. Sci. Part B: Polym. Phys.* **1996**, *34*, 545.

[123] Y. Peykova, O. V. Lebedeva, A. Diethert, P. Müller-Buschbaum, N. Willenbacher, *Int. J. Adhes. Adhes.* **2012**, *34*, 107.

[124] T. Tsukatani, Y. Hatano, H. Mizumachi, *J. Adhes.* **1989**, *31*, 59.

[125] C. A. Dahlquist, in *Treatise on Adhesion and Adhesives* (Ed: R. L. Ratrick), Dekker Publishing, New York, NY **1969**, p. 219.

[126] A. V. Pocius, *Adhesion and Adhesives Technology*, Carl Hanser, Munich, Germany **2012**.

[127] S. Abbott, *Adhesion Science: Principles and Practice*, DEStech Publications, Lancaster, PA **2015**.

[128] C. Derail, A. Allal, G. Marin, P. Tordjeman, *J. Adhes.* **1997**, *61*, 123.

[129] C. S. Lopes, Z. Gürdal, P. P. Camanho, *Comput. Struct.* **2008**, *86*, 897.

[130] B. Denkena, C. Schmidt, P. Weber, *Proc. Manuf. (MIC 2016)*, 6 **2016**, p. 96.

[131] A. Chiche, P. Pareige, C. Creton, C. R. Acad, *Sci. Ser. IV – Phys.* **2000**, *1*, 1197.

[132] O. Ben-Zion, A. Nussinovitch, *J. Adhes. Sci. Technol.* **2002**, *16*, 599.

[133] A. J. Kinloch, *Adhesion and Adhesives: Science and Technology*, Springer, Amsterdam, the Netherlands **2012**.

[134] D. Andrews, G. Scholes, G. Wiederrecht, *Comprehensive Nanoscience and Technology*, Elsevier Science, Amsterdam, the Netherlands **2010**.

[135] A. J. Stone, *The Theory of Intermolecular Forces*, OUP, Oxford **2013**.

[136] R. W. Jones, Y. Ng, J. F. McClelland, *Compos. Part A* **2008**, *39*, 965.

[137] E. B. Stark, A. M. Ibrahim, T. E. Munns, J. C. Seferis, *J. Appl. Polym. Sci.* **1985**, *30*, 1717.

[138] O. de Andrade Raponi, R. de Andrade Raponi, G. Bissaro Barban, R. M. di Benedetto, A. Carlos Ancelotti Jr.., *Mater. Res.* **2017**, *20*, 291.

[139] J. Hwan Shin, D. Kim, T. Centea, S. R. Nutt, *Compos. Part A* **2019**, *119*, 154.

[140] S. L. Agius, K. J. C. Magniez, B. L. Fox, *Compos. Part B* **2013**, *47*, 230.

[141] L. K. Grunenfelder, S. R. Nutt, *Compos. Sci. Technol.* **2010**, *70* (16), 2304.

[142] M. Akay, S. K. A. Mun, A. Stanley, *Compos. Sci. Technol.* **1997**, *57*, 565.

[143] P. Moy, F. E. Karasz, *Polym. Eng. Sci.* **1980**, *20*, 315.

[144] L. Li, M. Tirrell, G. A. Korba, A. V. Pocius, *J. Adhes.* **2001**, *76*, 307.

[145] D. Sowa, Z. Czech, Ł. Byczyński, *Int. J. Adhes. Adhes.* **2014**, *49*, 38.

[146] S. D. Tobing, A. Klein, *J. Appl. Polym. Sci.* **2001**, *79*, 2558.

[147] I. Khan, B. T. Poh, *J. Polym. Environ.* **2011**, *19*, 793.

[148] Z. Czech, R. Pełech, *Prog. Org. Coat.* **2010**, *67*, 72.

[149] I. Webster, *Int. J. Adhes. Adhes.* **1997**, *17*, 69.

[150] D. H-J, A. Lukaszewicz, K. Potter, *Proc. Inst. Mech. Eng.* **2012**, *226*, 193.

[151] K. S. Cho, *Viscoelasticity of Polymers: Theory and Numerical Algorithms*, Springer, Amsterdam, the Netherlands **2016**.

[152] J. D. Ferry, *Viscoelastic Properties of Polymers*, John Wiley & Sons, New York, NY **1980**.

[153] D. H. Kaelble, *J. Adhes.* **1969**, *1*, 102.

[154] M. F. Tse, L. Jacob, *J. Adhes.* **1996**, *56*, 79.

[155] E. P. Chang, *J. Adhes.* **1991**, *34*, 189.

[156] J. Chopin, R. Villey, D. Yarusso, E. Barthel, C. Creton, M. Ciccotti, *Macromolecules* **2018**, *51*, 8605.

[157] J. Du, D. D. Lindeman, D. J. Yarusso, *J. Adhes.* **2004**, *80*, 601.

[158] I. K. Mohammed, M. N. Charalambides, A. J. Kinloch, *J. Non-Newtonian Fluid Mech.* **2016**, *233*, 85.

[159] A. Forghani, C. Hickmott, H. Bedayat, C. Wohl, B. Grimsley, B. Coxon, A. Poursartip, SAMPE 2017, Seattle, WA **2017**.

[160] A. Forghani, C. Hickmott, H. Bedayat, C. Wohl, B. Grimsley, B. Coxon, A. Poursartip, Proc. ASC 32nd Ann. Techn. Conf., West Lafayette, IN **2017**.

[161] A. Forghani, C. Hickmott, V. Hutten, H. Bedayat, C. Wohl, B. Grimsley, B. Coxon, A. Poursartip, SAMPE 2018, Long Beach, CA **2018**.

[162] V. Hutten, A. Forghani, P. Silva, C. Hickmott, T. Sreekantamurthy, C. Wohl, B. Grimsley, B. Coxon, A. Poursartip, SAMPE 2019, Charlotte, NC **2019**.

[163] S. H. Dillman, J. C. Seferis, *J. Macromol. Sci. Part A: Chem.* **1989**, *26*, 227.

[164] E. M. Woo, J. C. Seferis, R. S. Schaffnit, *Polym. Compos.* **1991**, *12*, 273.